Environmental Engineering and Management Journal *February 2020, Vol. 19, No. 2, 235-245*
http://www.eemj.icpm.tuiasi.ro/; http://www.eemj.eu

"Gheorghe Asachi" Technical University of Iasi, Romania

COMPARATIVE STUDIES REGARDING MOLYBDATE ADSORPTION ONTO Mg_nFe LAYERED DOUBLE HYDROXIDES OBTAINED FROM REAGENT AND WASTE SLUDGE

Alin Golban, Lavinia Lupa, Laura Cocheci, Rodica Pode*

Politehnica University Timisoara, Faculty of Industrial Chemistry and Environmental Engineering, 6 Vasile Parvan Blvd., 300223, Timisoara, Romania

Abstract

Molybdate anions are used in a lot of fields and represent an essential trace element for plant and animal life; however, excessive amounts can cause adverse effect on various organism and environment. Therefore, in the present paper the adsorption performance of Mg_nFe- layered double hydroxides in the removal process of molybdate from aqueous solutions was studied. The layered double hydroxide (LDH) was synthesized by co-precipitation at low oversaturation method. Different ratio between Mg and Fe ions was used (Mg:Fe = 2:1; 3:1 and 4:1). The studied Mg_nFe- layered double hydroxides were synthesized starting from reagent and from iron waste sludge resulted from hot-dip galvanizing industry. In the removal process of molybdate from aqueous solutions were used the as-obtained and calcined at 450 °C adsorbents. The structural and morphological characterization of the obtained samples were made using BET (Brunauer-Emmett-Teller) analysis method, X-ray diffraction (XRD) and Scanning electron microscopy (SEM). The LDH materials obtained from an industrial waste have structural characteristics and similar or even higher adsorptive performance, as compared to those obtained from analytical grade reagents. Therefore, the approached LDH synthesis method, starting from secondary resources, represents a viable, affordable, and green route. This can successfully replace the expensive and resource-intensive traditional synthesis method, leading to cost reduction and valuable benefits in terms of environmental protection.

Key words: adsorption, layered double hydroxide, molybdate

Received: January, 2019; Revised final: January, 2020; Accepted: January, 2020; Published in final edited form: February, 2020

1. Introduction

Layered double hydroxides (LDH) with the general formula $[M(II)_{1-x}M(III)_x(OH)_2]^{x+}$ $(A^{n-}_{x/n})$ mH_2O, are synthetic anionic clays, which attracted a lot of interest due to their specific properties (Cavani et al., 1991). Their structure is formed from divalent ionic metals (e.g. Mg^{2+}, Zn^{2+}, Fe^{2+}) placed in the form of brucite-type layers, part of them being substitute by trivalent ions (e.g. Al^{3+}, Fe^{3+}) leading to positively charged layers. In the interlayers are found organic or inorganic anions which assure the molecules electroneutrality, conjugated with water molecules. Their layered structure confers best applies of these materials as ion exchangers, molecular sieves, catalysts or catalyst supports, biosenzors and sorbents (Benselka-Hadj Abdelkader et al., 2011; Kamiyama et al., 2016; Fahami and Beall, 2016; Zhang et al., 2014, Gilea et al., 2019). Due to their manageability interlayer region and due to their fluffy structure, these types of compounds are intensively used in the removal process of different pollutants from various environment samples (Turk et al., 2009). In general, for synthesizing LDHs compounds the most commonly used method is co-precipitation at a constant or variable pH by using pure chemical reagents that are rather expensive, or by using secondary sources of waste from different types of industries (Meng et al., 2016). A potential industry, which produces a significant amount of waste that

* Author to whom all correspondence should be addressed: e-mail: rodica.pode@upt.ro

could be used as secondary sources for LDHs obtaining is represented by the hot-dip galvanizing industry. One efficient method for using this waste is chemical extraction of valuable materials by using different organic or inorganic acid (acetic or citric acid, H_2NO_3, HCl, H_2SO_4) (Chou et al., 2010; Gheju et al., 2011; Shin et al., 2009; Xie et al., 2009). Therefore, in this study the iron sludge resulted from hot-dip galvanizing industry was used as secondary source of iron for the obtaining of Mg_nFe- layered double hydroxides (n = 2, 3 and 4). The aim of this work is to compare the structural properties of the obtained LDHs from secondary sources with those of the similar samples obtained from reagents. Besides structural properties, also the adsorption performance of the synthesised samples was also compared. In this aim as target pollutant, which to be retained by the studied materials, was chosen to be molybdenum (Mo). Molybdenum has many applications such as: micronutrient, corrosion inhibitors and alloying element. (Ardau al., 2012; Paikaray et al., 2013). At the same time, if it is present at higher concentration than it is recommended it can be harmful for human life (World Health Organization (Namasivayam and Sengeetha, 2006; WHO, 2011;). From this reason the development of new, efficient and less expensive method for molybdenum removal or recover from various aqueous solution always represent a challenge.

2. Experimental

2.1. Adsorbent obtaining and characterization

The synthesis method for Mg_nFe - layered double hydroxides consist in co-precipitation at low oversaturation, as described by Cavani et al., 1991. The sludge used for obtaining of iron precursor was received from a local hot-dip galvanizing plant. The dissolution of iron sludge was detailed in our previous published work (Goban et. al., 2018) the optimum condition of iron ions extraction from sludge being: 20% sulfuric acid solution, solid:liquid ratio 1:1.2 and a contact time between the two phases of 60 minutes. In the resulted iron precursor solution, the iron concentration is of 84 g/L and the Zn ions have a concentration of 2.38 g/L. The other ions present in the sludge were extracted in a smaller amount due to the formation of calcium and lead sulphates, which are hardly soluble.

A calculated amount of solution, obtained from acid dissolution of sludge, was used as precursor of the trivalent cation (iron) for, Mg_nFe -S synthesis or $Fe(NO_3)_3 \cdot 9H_2O$ analytical grade reagent for preparation of a blank sample - Mg_nFe -R. A measured amount of $Mg(NO_3)\cdot 6H_2O$ analytical grade reagent was also used, in order to obtain different molar ratio of Mg/Fe (n = 2, 3 and 4). This solution was added dropwise to a 1 M solution of Na_2CO_3, under vigorous magnetic stirring and keeping the pH value to 11.5 by means of 2 M NaOH solution. The brown-red precipitate was maintained under stirring for 2 h in order to finish the incorporation of cations solution, and then aged at 70 °C for 18 h, washed several times with distilled water in order to remove the unreacted substances, filtered and dried at 70°C over night. The obtained samples were crushed to powders and sieved. The calcined samples were heated at 450 °C using a rate of 10 °C/min. A Nabertherm oven was used for the sample calcination.

The structural and morphological characterization of the Mg_nFe layered double hydroxides, obtained from both sources: iron sludge and also analytical grate reagents, were made using X-ray diffraction (XRD), scanning electron microscopy (SEM) and BET (Brunauer-Emmett-Teller) analysis.

A Rigaku Ultima IV X-ray diffractometer was used for the XRD analyse. SEM images were register with a Quanta FEG 250 microscope. The BET analysis method used to determine the specific surface area and pore volume were determined by N_2 adsorption-desorption at 77 K, using, with a Micromeritics ASAP 2020 instrument.

2.2. Sensitivity analysis Mo(VI) adsorption

For the adsorption of Mo(VI) on the studied samples, a stock solution of 1 g/L Mo(VI) was prepared using ammonium molybdate tetrahydrate $(NH_4)_6Mo_7O_{24}\cdot 4H_2O$. All adsorption experiments were performed by contacting 25 mL of solutions containing Mo(VI) with the adsorbents samples corresponding to a solid:liquid ratio of 1g/L. The Mo(VI) removal was conducted in a batch shaker model Julabo, to reach the adsorption equilibrium. At equilibrium, the solid was separated by filtration and the residual concentration of Mo(VI) ions was analysed by atomic adsorption spectrophotometer (Varian SpectrAA 280 FS).

Different initial pH values (4, 6, 8, 10) of a 30 mg/L Mo(VI) solution were used to determine the pH effect upon the adsorption efficiency. The pH value was modified by using 1 mol/L NaOH or 1 mol/L HCl, and the pH was determined with a Mettler Toledo pH-meter. To determine the effect of sorption time, different time intervals have been set (15-240 min).

Adsorption isotherm was conducted in the optimum conditions of pH and contact time established before, using solutions containing different initial concentrations of Mo(VI) (5, 10, 30, 50, 100 and 150 mg/L). The quantity of molybdate retained by the studied materials was calculated using the following Eq (1):

$$q_e = (C_0 - C_e)\, V/m \qquad (1)$$

where: q_e is the adsorption capacity of sorbent material at equilibrium (mg/g), V the volume of solution (L), C_0 (mg/L) and C_e (mg/L) the initial and equilibrium concentrations of Mo(VI), and m is the mass of adsorbent (g).

3. Results and discussions

3.1. Adsorbent characterization

The XRD patterns of the as-synthesised sample and calcined at 450°C are presented in Fig. 1 and can be observed that both the Mg_nFe - layered double hydroxides obtained from reagents and obtained from secondary sources correspond to the formula of pyroaurite: $Mg_6Fe_2CO_3(OH)_{16}{\cdot}4H_2O$ (DB card number 9009439). The use of solution obtained from acid dissolution of iron sludge as iron precursor doesn't lead to the obtaining of second phases or impurities in the synthesized samples. In case of the samples calcined at 450°C the layered structure collapses and the RX spectrum are specific for amorphous phases. From this reason it is expected that the samples calcined at 450 °C to develop higher adsorption capacity than the as-synthesized samples.

For the basal planes (0 0 3) and (0 0 6) the corresponding reflexions are found at low 2θ angles, while for the non-basal planes (0 1 2), (0 1 5), (0 1 8), (1 1 0) and (1 1 3), the corresponding reflexions are found at high 2θ angles. The values of 2θ angles corresponding to the basal and non-basal planes of the as-synthetized samples, and the calculated basal spacing are presented in Table 1. The values of the basal spacing $d_{(0\,0\,3)}$ are close to each other and correspond to carbonate interlayer pyroaurites. Also, the values of $d_{(1\,1\,0)}$ spacing are typical for Mg-Fe layered double hydroxides, as presented in literature data (Ahmed and Gasser, 2012; Vucelic et. al, 1997)

Fig. 2. shows the SEM images of the synthesised LDH both from reagents and secondary sources. It can be observed that both the materials obtained from secondary sources and from reagent present similar morphology as fluffy particles staked in overlaid layers. This aerated structure is more evident with the increasing of the Mg/Fe molar ratio. Through calcination at 450 °C the samples are more amorphous presenting a cotton appearance (Fig. 2).

The values resulted from the BET analysis regarding the specific surface area and the pore volume of the studied sample are listed in Table 2.

For all the samples (obtained from reagents or from secondary sources) it can be observed that by increasing the molar ratio Mg/Fe lead to a slide increasing of the specific surface area. The calcinated samples present almost a double surface area than their precursors.

Considering the morphological structure of the sample it is expected that the adsorption capacity developed in the removal process of Mo(VI) from aqueous solutions to increase with the Mg/Fe molar ratio increasing and to be much higher for the calcinated samples.

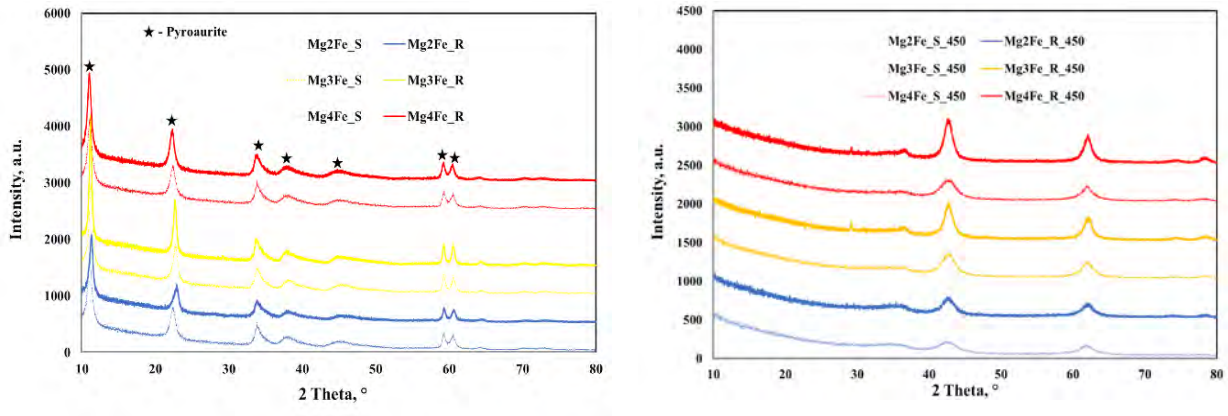

(a) (b)

Fig. 1. XRD pattern of: a) Mg_nFe as-synthesised and b) Mg_nFe - calcinated at 450 °C

Table 1. Values of 2θ angles for the basal and non-basal planes of as-synthetized samples

	Mg_2Fe-R	***Mg_2Fe-S***	***Mg_3Fe-R***	***Mg_3Fe-S***	***Mg_4Fe-R***	***Mg_4Fe-S***
$d_{(0\,0\,3)}$ (Å)	7.90	7.81	7.82	7.83	8.02	7.98
$d_{(1\,1\,0)}$ (Å)	1.56	1.57	1.56	1.56	1.57	1.56
(h k l) plane	**2θ (°)**					
(0 0 3)	11.04	11.30	11.17	11.21	11.00	11.05
(0 0 6)	23.04	22.92	22.64	22.71	22.24	22.33
(0 1 2)	38.42	38.52	37.68	38.30	37.58	37.64
(0 1 5)	45.10	45.08	44.78	44.89	44.40	44.52
(0 1 8)	59.28	59.30	59.20	59.25	59.10	59.20
(1 1 0)	60.61	60.66	60.50	60.57	60.35	60.48
(1 1 3)	72.77	72.84	72.51	72.96	72.66	72.58

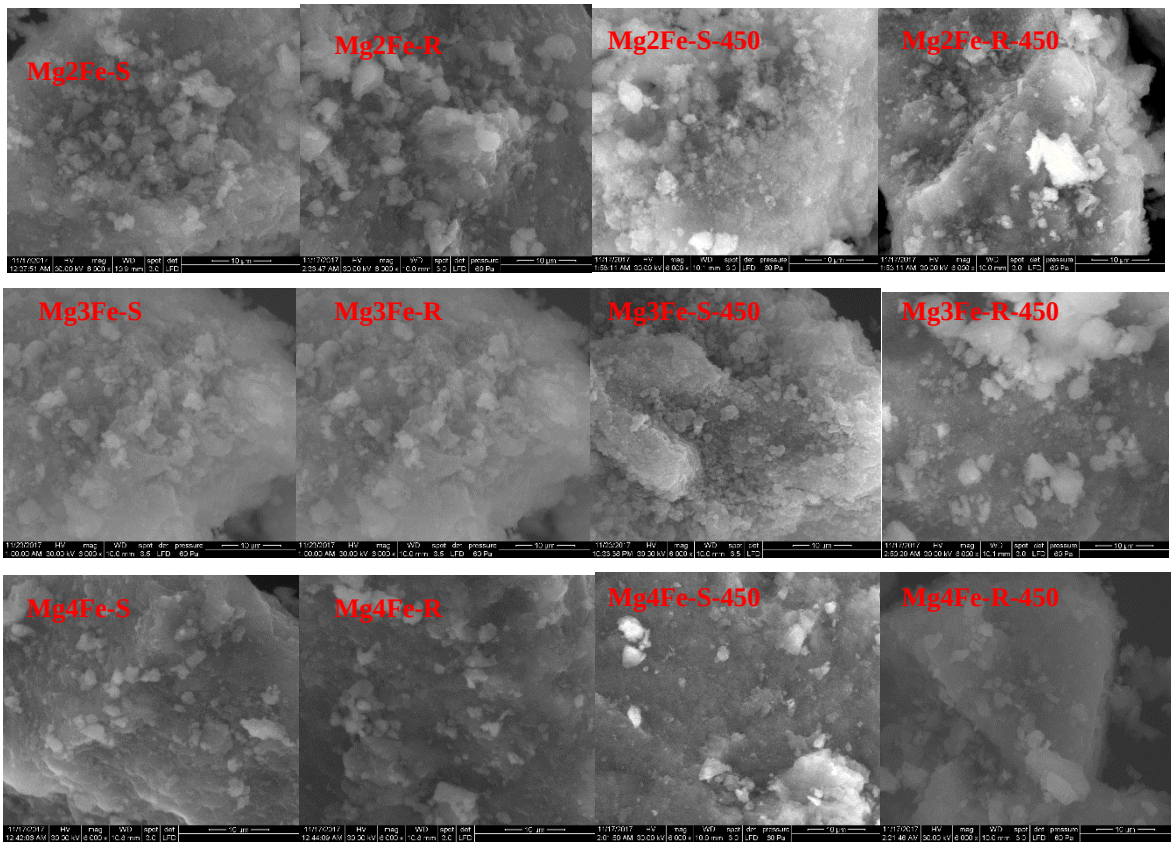

Fig. 2. SEM images of the Mg_nFe - LDH as-synthesised and calcinated at 450 °C

Table 2. Specific surface area and pore volume

Adsorbent material	S_{BET} (m^2/g)	V_p (cm^3/g)
Mg2Fe-S	64.2	0.64
Mg2Fe-R	44.2	0.41
Mg3Fe-S	73.4	0.56
Mg3Fe-R	50.7	0.50
Mg4Fe-S	98.9	0.53
Mg4Fe-R	83.3	0.44
Mg2Fe-S-450	130	0.75
Mg2Fe-R-450	121	0.60
Mg3Fe-S-450	144	0.78
Mg3Fe-R-450	132	0.64
Mg4Fe-S-450	189	0.82
Mg4Fe-R-450	170	0.66

3.2. Effect of pH upon the adsorption efficiency

The effect of the initial pH of the sample upon the adsorption capacity developed by the studied materials in the removal process of Mo(VI) from aqueous solutions are presented in Fig. 3. It can be observed that through increasing of the initial pH from 4 to 6 the adsorption capacity increase obtaining a maximum at pH 6. At this pH value the Mo(VI) are present in solution only as molybdate anion (MoO_4^{2-}) (Tkac and Paulenova 2008). At higher pH there is a competition between the molybdate anion (MoO_4^{2-}) and the hydroxyl anions (HO^-) present in solution, which lead to a decreasing of the obtained adsorption capacities. Therefore, for the subsequent experiments a pH value of 6 was selected.

3.3. Effect of contact time on the adsorption efficiency

The behaviour of adsorption capacity of the studied materials in the removal process of Mo(VI) from aqueous solutions function of time is presented in Fig. 4. It can be observed that the equilibrium between the adsorbent and molybdate anion is achieved in 60 minutes for all the studied materials, this being considered the work time for the following experiments.

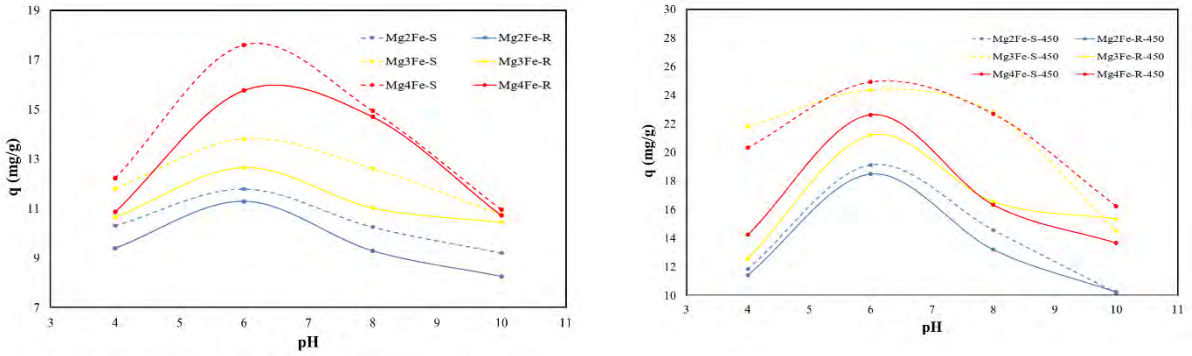

a) Mg_nFe as-synthesised b) Mg_nFe - calcined at 450 °C

Fig. 3. Effect of initial pH on the adsorption capacity of the studied materials in the removal process of Mo(VI) ions from aqueous solutions

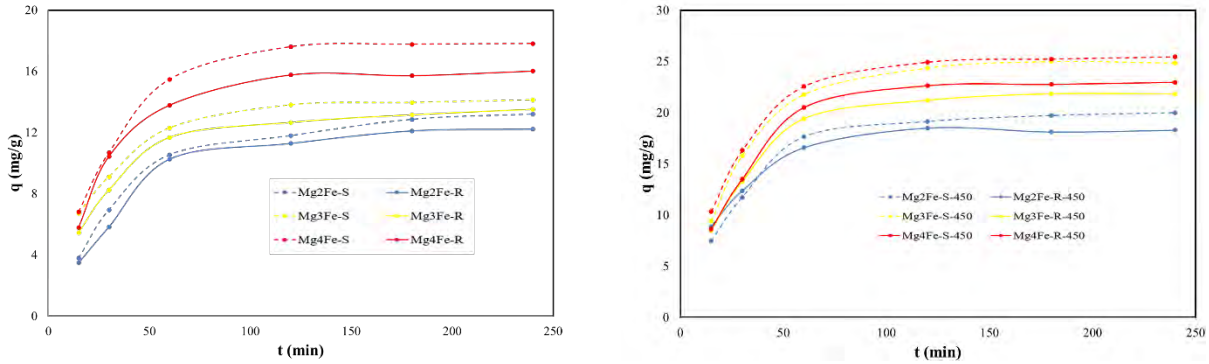

a) Mg_nFe as-synthesised b) Mg_nFe - calcined at 450 °C

Fig. 4. Effect of contact time on the adsorption capacity of the studied materials in the removal process of Mo(VI) ions from aqueous solutions

The experimental data regarding the dependence of the adsorption capacity of the studied materials function of contact time were used for kinetic modelling. In this way three kinetic models: pseudo-first-order equation, pseudo-second-order reaction model and intra-particle diffusion model, were discussed. The pseudo-first-order kinetic model is defined by the Equation: (Ardau et al. 2012; Haro et al. 2017; Namasivayam and Sengeetha 2006).

$$\ln(q_e - q_t) = \ln q_t - k_1 \cdot t \qquad (2)$$

where: q_e and q_t are the amount of the Mo(VI) adsorbed onto the studied materials (mg/g) at equilibrium and after time t, respectively. t is the contact time (min), k_1 is the specific sorption rate constant (min^{-1}).

The values of the adsorption rate constant (k_1) were determined from the plot of $ln\ (q_e - q_t)$ versus t (Fig. 5). The linear form of the pseudo-second order model based on the solid phase adsorption and implying that the chemisorption is the rate controlling step is defined by: (Ardau et al., 2012; Namasivayam and Sengeetha, 2006; Haro et al., 2017).

$$\frac{t}{q_t} = \frac{1}{k_2 \cdot q_e^2} + \frac{t}{q_e} \qquad (3)$$

where: q_e and q_t are the amount of the Mo(VI) adsorbed onto the studied materials (mg/g) at equilibrium and at time t, respectively. t is the contact time (min), k_2 is the pseudo-second-order adsorption rate constant (g/(mg·min)). The value q_e and k_2 are determined from the slope and intercept of (t/q_t) versus t (Fig. 6.).

In order to determine the rate-limiting step in the process of molybdate adsorption onto the studied materials, intra-particle diffusion model was studied. This step could be controlled by boundary layer dispersion or intra-particle (pore) dispersion of solute towards the solid surface. The Weber-Morris ecuation was used to identify the possibility of intra-particle diffusion resistance:

$$q_t = k_{int} \cdot t^{1/2} + C \qquad (4)$$

where: k_{int} is the intra-particle diffusion rate constant ($mg/g \cdot min^{1/2}$) and C is the intercept. The values of q_t versus $t^{1/2}$ and the rate constant k_{int} are directly evaluated from the slope of the regression line (Fig. 7).

The values of the constants, together with the regression coefficients (R^2) obtained in all cases are summarized in Table 3.

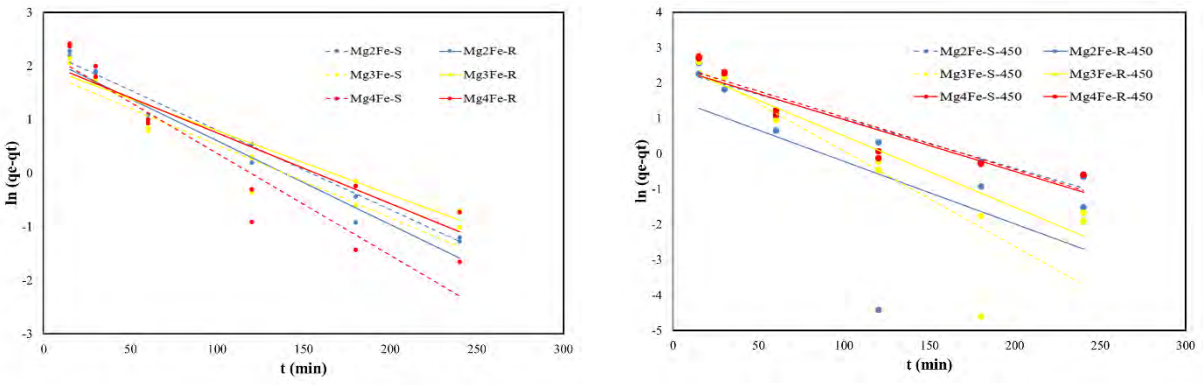

Fig. 5. Pseudo-first order kinetic models for Mo(VI) adsorption onto the studied materials

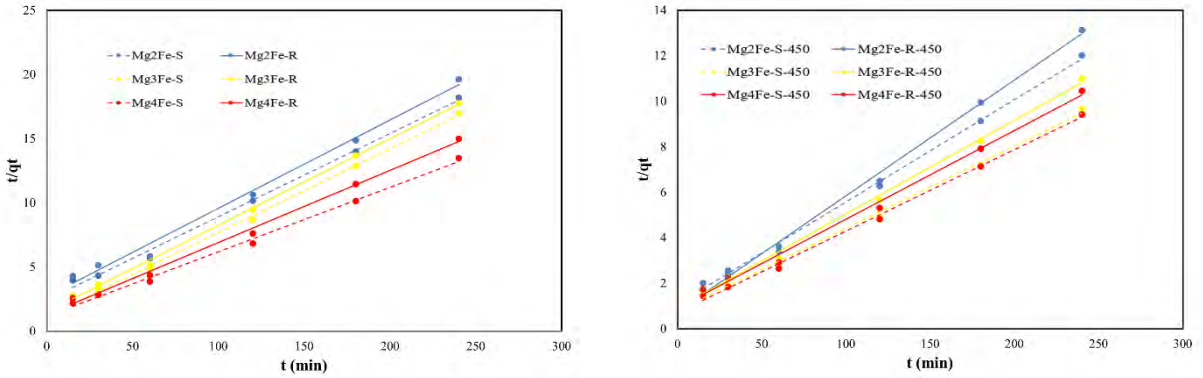

Fig. 6. Pseudo-second order kinetic model for Mo(VI) adsorption onto the studied materials

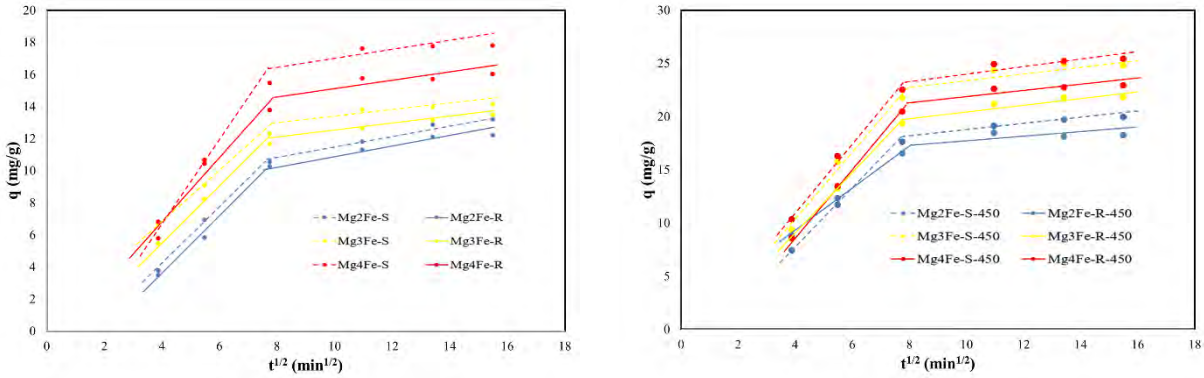

Fig. 7. Intraparticle diffusion of Mo(VI) onto the studied materials

Table 3. Kinetic parameters for Mo(VI) sorption onto the studied materials

Adsorbent material	$q_{e,exp}$ *mg Mo(VI) /g*	*Pseudo-first-order model*			*Pseudo-second-order model*			*Intraparticle diffusion*	
		$q_{e,calc}$, *mg/g*	k_1,*min*$^{-1}$	R^2	$q_{e,calc}$, *mg/g*	k_2, *min/(mg/g)*	R^2	k_{int}	R^2
Mg_2Fe-S	13.5	9.86	0.0142	0.9831	15.6	0.00172	0.9952	1.73	0.9952
Mg_2Fe-R	12.5	8.71	0.0156	0.9538	14.5	0.00182	0.9907	1.76	0.9941
Mg_3Fe-S	14.5	6.59	0.0132	0.9041	15.4	0.00376	0.9982	1.44	0.9984
Mg_3Fe-R	14.0	7.24	0.0108	0.9318	14.8	0.00314	0.9986	1.60	0.9974
Mg_4Fe-S	18.0	9.63	0.0189	0.8995	20.0	0.00221	0.9957	2.23	0.9976
Mg_4Fe-R	16.5	7.90	0.0132	0.8623	17.8	0.00258	0.9958	2.03	0.9632
Mg_2Fe-S-450	20.5	10.7	0.0126	0.9168	22.7	0.00183	0.9958	2.63	0.9997
Mg_2Fe-R-450	18.5	4.72	0.0169	0.4048	20.0	0.00346	0.9968	1.98	0.9982
Mg_3Fe-S-450	25.0	15.8	0.0268	0.8904	27.8	0.00163	0.9957	3.16	0.9863
Mg_3Fe-R-450	22.0	12.4	0.0192	0.9254	24.4	0.00195	0.9959	2.80	0.9986
Mg_4Fe-S-450	26.0	12.1	0.0136	0.8892	28.6	0.00174	0.9967	3.13	0.9924
Mg_4Fe-R-450	23.5	11.3	0.0138	0.8563	25.6	0.00176	0.9949	3.07	0.9995

Due to the fact that in case of the pseudo-first-order equation the experimental data are far apart from the linearity, obtaining poor regression coefficients and because there is a discrepancy between the q_e values experimentally obtained and the values obtained directly from the kinetic plot (Fig. 5.) can be mentioned that this kinetic model does not describe the Mo(VI) adsorption onto the studied materials. In all the cases the correlation coefficients for the linear plot of the pseudo-second-order kinetic plot is excellent, greater than 0.99. In the same time the values obtained for the adsorption capacity obtained experimentally and from the kinetic plot are very close. Therefore, can be concluded that the Mo(VI) adsorption onto the studied materials is best described by the pseudo-second order kinetic model. As respect for the intra particle diffusion, it can be observed that the Mo(VI) adsorption onto the studied materials present a complex mechanism which take place in two steps: the first linearity represents the distribution of adsorbate through the solution to the external surface of adsorbent, and the second one could be attributed to the gradual adsorption stage, where intraparticle diffusion is rate limiting (Cong and Jianping, 2018).

3.4. Effect of Mo(VI) initial concentration on the adsorption efficiency

The equilibrium isotherm of the Mo(VI) adsorption onto the studied materials are presented in Fig. 8. The adsorption capacities developed by the studied materials increase with the increasing of the equilibrium concentration, until it reaches a constant value which represent the saturation of the adsorbent with the molybdate anions.

In order to determine the maximum adsorption capacities of the studied materials the experimental data were fitted with the following isotherms: Langmuir, Freundlich, Temkin and Dubinin-Radushkevich (Abubeah et al., 2018). The Langmuir isotherm is described by the following equation in its linear form: (Xiaoliang et al., 2017)

$$\frac{C_e}{q_e} = \frac{1}{K_L \cdot q_m} + \frac{C_e}{q_m} \tag{5}$$

where: q_e is the amount of Mo(VI) uptake per gram of adsorbent (mg/g), and C_e is the equilibrium concentration of adsorbate in the bulk solution after adsorption (mg/L). q_m is the measure of the monolayer sorption capacity (mg/g) and K_L denotes the Langmuir isotherm constant related to the affinity between adsorbent and the adsorbate (L/mg). From the plot of C_e/q_e versus C_e presented in Fig. 9 there were determined the Langmuir parameters which are showed in Table 2. Eq. (6) is the linear form of the Freundlich equation (Wang et al., 2018),

$$ln\, q_e = ln\, K_F + \frac{1}{n} ln\, C_e \tag{6}$$

where: K and $1/n$ are characteristic constants that can be related to the relative adsorption capacity of the adsorbent (mg/g) and the intensity of the adsorption, respectively. These parameters listed in Table 4 were determined from the slope and intercept of the linear plot of lnq_e against C_e (Fig. 10).

The interactions between adsorbent-adsorbate could be described by the linear equation of Temkin isotherm: (Johnson and Arnold, 1995)

$$q_e = \frac{RT}{b} \ln k_T + \frac{RT}{b} \ln C_e \tag{7}$$

where: T is the absolute temperature (K), R is the gas constant, K_T (L/mg) is the equilibrium binding constant corresponding to the maximum binding energy, b (kJ/mol) is Temkin isotherm constant, RT/b (dimensionless) is related to the heat adsorption. K_t and b can be calculated from the slope and intercept of the linear plot of q_e versus lnC_e (Fig. 11.) and the results together with the regression coefficient are listed in Table 4.

The D-R isotherm model in its linear form was tested to establish the mechanism type of Mo(VI) adsorption (physical or chemical) onto the studied materials: (Hu and Zhang, 2019).

$$\ln q_e = \ln q_s - K_{ad} \cdot \varepsilon^2 \tag{8}$$

where: q_e = amount of adsorbate in the adsorbent at equilibrium(mg/g); q_s = theoretical isotherm saturation capacity (mg/g); K_{ad} = Dubinin–Radushkevich isotherm constant (mol^2/kJ^2). ε can be correlated as given by Eq. (9):

$$\varepsilon = RT \ln\left[1 + \frac{1}{C_e}\right] \tag{9}$$

where: R, T and are the gas constant (8.314 J/mol.K), absolute temperature (K) and adsorbate equilibrium concentration (mg/L) respectively. The parameters specific for D–R isotherm were determined from the linear plot of lnq_e function of ε^2 (Fig. 12.) and were listed in Table 4.

The Langmuir isotherm showed a better design of the experimental data resulted during the adsorption of molybdenum onto the studied materials, than the rest of the isotherms. The fact that the Langmuir isotherm fits the experimental data well may be due to homogeneous distribution of active sites on the studied samples since the Langmuir equation estimates that the adsorbent outer is uniform charge. The maximum adsorption capacity developed by the studied materials increase with the molar ratio increasing between Mg and Fe from the synthesised LDH. The LDH synthesised from secondary sources present even slightly higher maximum adsorption capacity than the LDH obtained from reagents. The maximum adsorption capacities developed by the calcinated samples at 450°C are with 50% higher than those of their precursors.

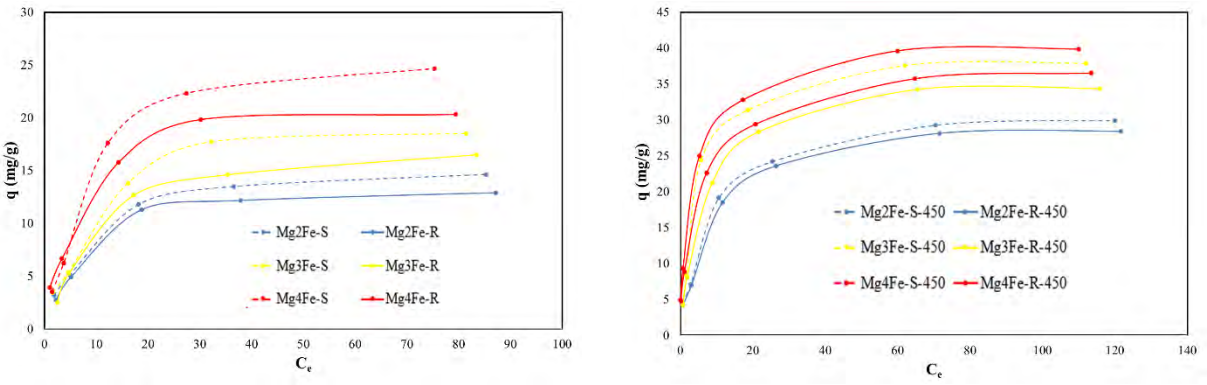

Fig. 8. Equilibrium isotherm of Mo(VI) adsorption onto the studied materials

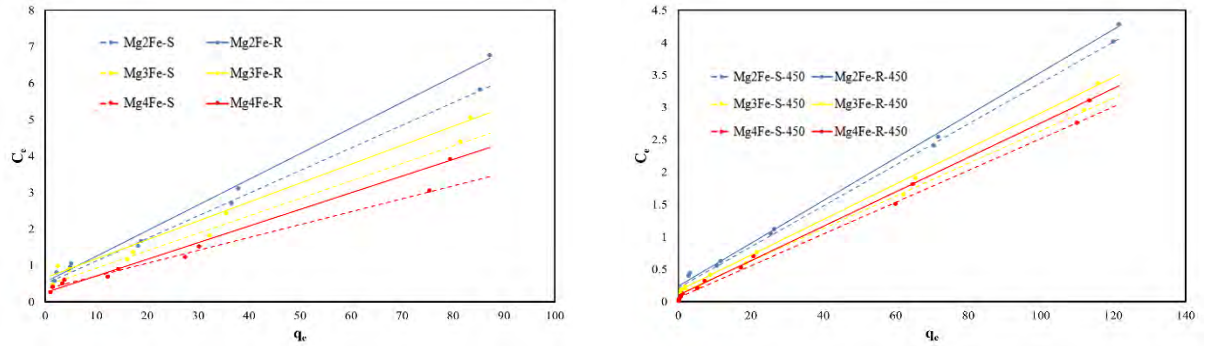

Fig. 9. Langmuir isotherm for Mo(VI) adsorption onto the studied materials

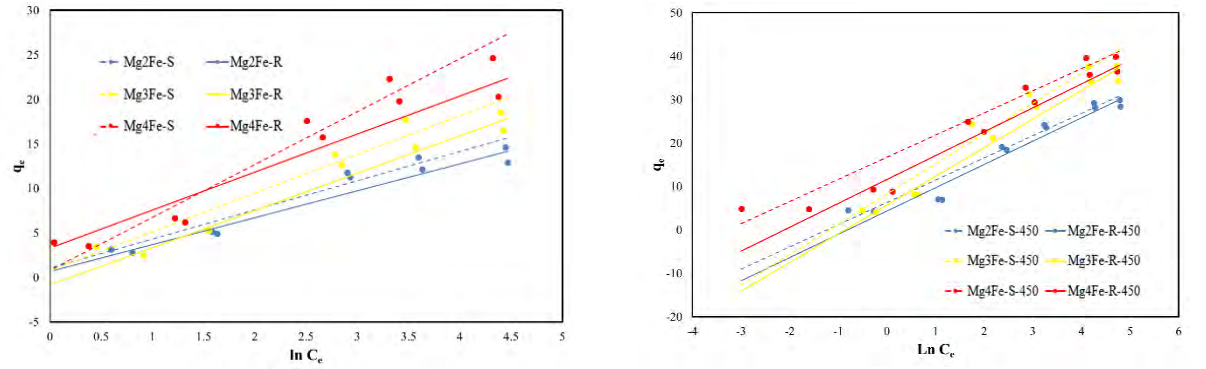

Fig. 10. Freundlich isotherm for Mo(VI) adsorption onto the studied materials

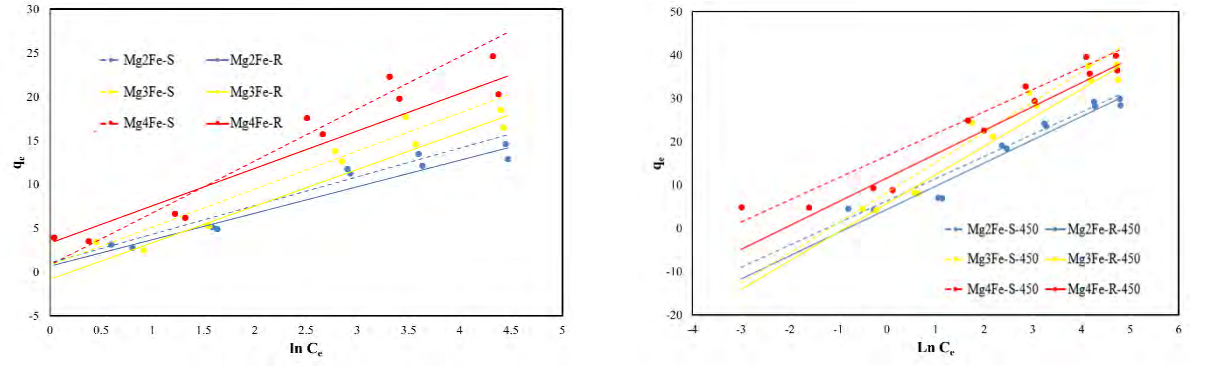

Fig. 11. Temkin isotherm for Mo(VI) adsorption onto the studied materials

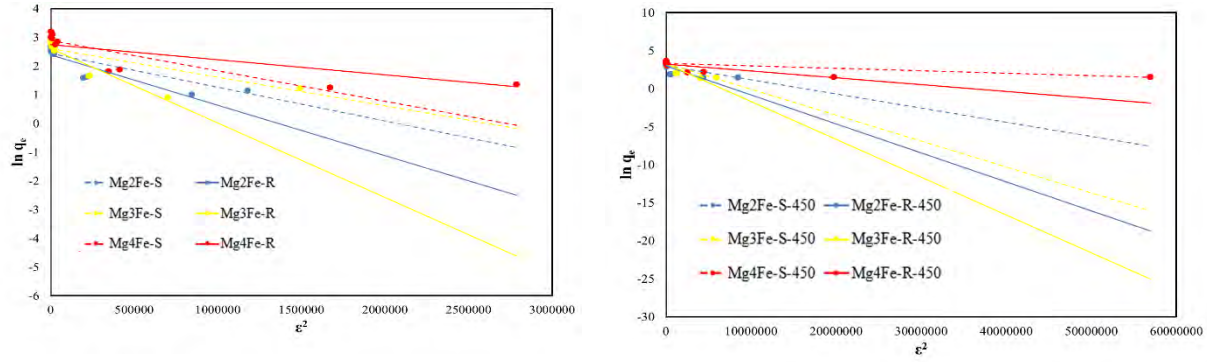

Fig. 12. Dubinin- Radushkevich isotherm for Mo(VI) adsorption onto the studied materials

Table 4. Equilibrium sorption isotherm parameters for Mo(VI) adsorption onto the studied materials

Studied materials	$q_{m\ exp}$, *mg/g*	*Langmuir*			*Freundlich*			*Temkin*			*Dubinin- Radushkevich*		
		K_L, *L/mg*	$q_{m\ calc}$, *mg/g*	R^2	K_F, *mg/g*	*1/n*	R^2	K_T, *L/g*	b_T, *J/mol*	R^2	K_{ad}, *mol²/kJ²*	q_s, *mg/g*	R^2
Mg_2Fe-S	14.6	0.124	16.1	0.9979	2.69	0.426	0.9379	24.8	755	0.9603	$1.24*10^{-6}$	12.1	0.7768
Mg_2Fe-R	12.9	0.127	14.2	0.9964	2.31	0.438	0.9019	99.5	820	0.9350	$2.53*10^{-6}$	10.9	0.8582
Mg_3Fe-S	18.5	0.109	20.9	0.9920	2.92	0.472	0.9337	290	570	0.9428	$1.34*10^{-6}$	13.7	0.7112
Mg_3Fe-R	16.5	0.0787	19.2	0.9926	2.01	0.534	0.8995	157	593	0.9695	$3.48*10^{-6}$	13.6	0.9259
Mg_4Fe-S	24.7	0.102	28.2	0.9931	3.33	0.528	0.9179	1863	417	0.9545	$1.46*10^{-6}$	18.0	0.7791
Mg_4Fe-R	20.3	0.181	21.9	0.9972	4.21	0.413	0.9385	3.67	579	0.9497	$5.27*10^{-7}$	15.6	0.7499
Mg_2Fe-S-450	30.0	0.151	31.5	0.9975	6.10	0.371	0.9391	2.25	485	0.9486	$2.28*10^{-7}$	20.2	0.6170
Mg_2Fe-R-450	28.5	0.137	30.3	0.9983	5.15	0.403	0.9362	3.42	463	0.9619	$4.18*10^{-7}$	20.1	0.6773
Mg_3Fe-S-450	37.9	0.206	39.7	0.9993	7.25	0.414	0.8800	2.34	355	0.9536	$3.49*10^{-7}$	28.1	0.7896
Mg_3Fe-R-450	34.5	0.163	36.5	0.9995	6.02	0.426	0.9151	3.19	376	0.9785	$5.47*10^{-7}$	26.2	0.8424
Mg_4Fe-S-450	39.9	0.422	39.4	0.9991	12.0	0.295	0.9611	1.35	487	0.9528	$3.26*10^{-8}$	27.2	0.6845
Mg_4Fe-R-450	36.6	0.265	338	0.9989	9.07	0.337	0.9605	1.60	451	0.9788	$9.05*10^{-8}$	25.5	0.7218

In the Langmuir equation K_L is used to classify the equilibrium parameter (R_L) using Eq. 10:

$$R_L = \frac{1}{1 + K_L C_0} \qquad (10)$$

where: K_L is the Langmuir constant and C_o is the initial concentration of Mo(VI) ions. The value of separation parameter R_L provides important information about the nature of adsorption. The value of R_L indicated the type of Langmuir isotherm to be irreversible (R_L =0), favourable (0< R_L< 1), linear (R_L=1), or unfavourable (R_L> 1) (Meroufel et al., 2013) The R_L was found to be between 0 and 1 for the entire concentration range, and for all the studied material which indicates the favourable adsorption of Mo(VI) onto the studied materials.

The Freundlich plots have a lower correlation coefficient. This suggests that the use of the Freundlich isotherm is limited. The 1/n parameter from the Freundlich plot point out also the attraction of the studied samples for Mo(VI) ions. If it is bellow one the affinity between these two is strong.

Temkin and D-R isotherms developed lower regression coefficient, therefore these two isotherms should be restrictively used for fitting the experimental data. The samples resulted after Mo(VI) adsorption were subjected to the XRD analysis in order to identify the adsorption mechanism of the Mo(VI) onto the studied samples.

The results are presented in Fig. 13, where from it is evident that, after Mo(VI) adsorption, the diffractograms of the studied materials did not suffer any changes, all the XRD patterns being characteristics for the pyroaurite group of layered double hydroxides. The calcined materials regained their layered structure after contacting the molybdate solution, the specific peaks of pyroaurite being present, with no evidence of molybdate anion presence in the interlayer space (the position of peaks and their intensities did not suffer substantial modifications).

This indicates that the molybdate anion didn`t displaced the carbonate anion from the interlayer space. It is well known that the displacement of carbonate anion from the layered double hydroxides structure is very difficult to achieve. Therefore, it is supposed that the retained mechanism of Mo(VI) onto the surface of the studied materials is its adsorption on the surface, due to the electrostatic interections between the positively charged brucite type layers and molybdate anions. The calcinated samples due tio the contacted with the molybdate solutions firstly regained their layered structure and then adsorbed the target anions. They developed a higher adsorption capacity due to their higher specific surface area.

Table 5 presents the maximum adsorption capacity, reported in literature, developed by different adsorbents in the removal process of Mo(VI) from aqueous solutions.

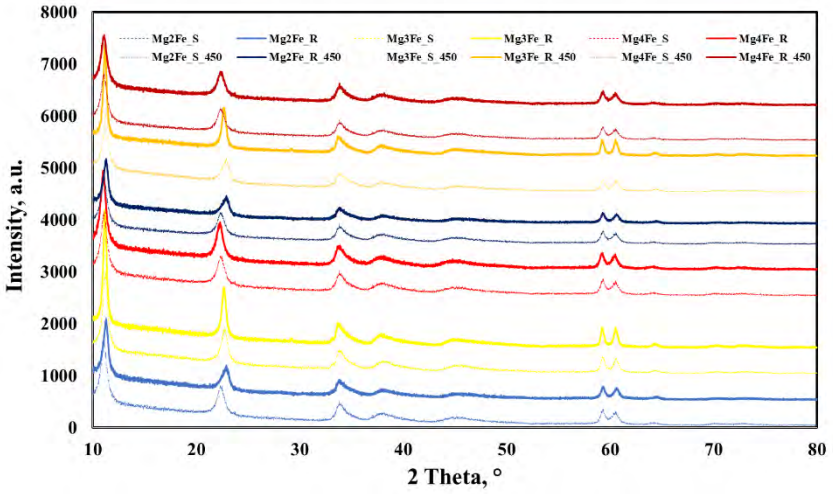

Fig. 13. XRD pattern of the studied samples after Mo(VI) adsorption

Table 5. The adsorption capacities of different adsorbents developed in the removal processes of MoO_4^{2-} ions from aqueous solutions

Adsorbent	q_m *(mg/g)*	*References*
Maghemite (γ-Fe_2O_3)	33.4	Afkhami and Norooz-Asl, 2009
$MgFeSO_4$-type HT-LDH	15.5	Paikaray et al., 2013
$ZnCl_2$ activated coir pitch carbon	18.9	Namasivayam and Sengeetha, 2006
Mg4Fe-S	24.7	Present paper
Mg4Fe-S-450	39.9	

It can be observed that the studied LDH structures present close or even higher efficiency than similar adsorbents reported in the literature.

4. Conclusions

This paper aimed the structural and adsorptive properties characterization of a Mg_nFe layered double hydroxide and its calcined product, to be used for molybdate Mo(VI) retention from waters.

The structural analysis by X-ray diffraction confirmed that the as-synthesized sample was a Mg_nFe - layered double hydroxides. The calcined LDH shows higher specific surface area and total pore volume than its LDH precursor.

The kinetic study of the adsorption showed that the process accurately obeyed pseudo-second order kinetics (correlation coefficients > 0.99). The results concerning the equilibrium of the process showed that the calcinated samples at 450°C exhibited better efficiency (maximum adsorption capacity 39.9 mg/g) in the adsorption process of Mo(VI) from aqueous solutions, than its precursor LDH (24.7 mg/g), in accordance with their specific surface area.

The correlation of the techniques used for the characterization of the obtained LDH, before and after molybdate adsorption, lead to the conclusion that the LDH materials obtained from an industrial waste have structural characteristics and similar or even higher adsorptive performance, as compared to other materials obtained from expensive analytical grade reagents reported in the literature. Therefore, the approached LDH synthesis method, starting from secondary resources, represents a viable, affordable, and green route. This can successfully replace the expensive and resource-intensive traditional synthesis method, leading to cost reduction and valuable benefits in terms of environmental protection.

The use of iron sludge as an alternative sources of iron ions for the synthesis of Mg_nFe – LDH represent an advantage for both economic and environmental protection point of view.

Acknowledgements

The studies were done during the PhD program from the Doctoral School of the University Politehnica Timisoara.

References

Abubeah R., Altaher H., Khalil T.E., (2018), Removal of hexavalent chromium using two innovative adsorbents, *Environmental Engineering and Management Journal,* **17,** 1621-1634.

Afkhami, A., Norooz-Asl, R., (2009), Removal, preconcentration and determination of Mo(VI) from water and wastewater samples using maghemite nanoparticles, *Colloids and Surfaces A: Physicochemical and Engineering Aspects*, **346**, 52-57.

Ahmed, I.M., Gasser, M.S., (2012), Adsorption study of anionic reactive dye from aqueous solution to Mg–Fe–CO_3 layered double hydroxide (LDH), *Applied Surface Science*, **259**, 650-656.

Ardau C., Frau F., Dore E., Lattanzi P., (2012), Molybdate sorption by Zn-Al sulphate layered double hydroxides, *Applied Clay Science*, **65-66**, 128-133.

Benselka-Hadj Abdelkadera N., Bentouami A., Derrichea Z., Bettahara N., de Menorval L.-C, (2011), Synthesis and characterization of Mg–Fe layer double hydroxides and its application on adsorption of Orange G from aqueous solution, *Chemical Engineering Journal*, **169**, 231-238.

Cavani F., Trifiro F., Vaccari A., (1991), Hydrotalcite-type anionic clays: preparation, properties and applications, *Catalysis Today*, **11**, 173-301.

Chou J.D., Lin C.L., Wey M.Y., Chang S.H., (2010), Effect of Cu species on leaching behavior of simulated copper sludge after thermal treatment: ESCA analysis, *Journal of Hazardous Materials*, **179**, 1106-1110.

Cong L., Jianping C., (2018), Potential role of intraparticle diffusion in dynamic partitioning of secondary organic aerosols, *Atmospheric Pollution Research*, **9**, 1131-1136.

Fahami A., Beall G., (2016), Structural and morphological characterization of $Mg_{0.8}Al_{0.2}(OH)_2Cl_{0.2}$ hydrotalcite produced by mechanochemistry method, *Journal of Solid State Chemistry*, **233**, 422–427.

Gheju M., Pode R., Manea F., (2011), Comparative heavy metal chemical extraction from anaerobically digested biosolids, *Hydrometallurgy,* **108**, 115-121.

Gilea D., Lutic D., Carja G., (2019), Heterostructures of silver and zinc based layered double hydroxides for pollutant removal under simulated solar light, *Environmental Engineering and Management Journal,* **18**, 1765-1772.

Golban A., Cocheci L., Lazau R., Lupa L., Pode R., (2018), Iron ions reclaiming from sludge resulted from hot-dip galvanizing process, as Mg3 Fe-layered double hydroxide used in the degradation process of organic dyes, *Desalination and Water Treatment,* **131**, 317-327.

Haro N.K., Del Vecchio P., Marcilio N.R., Feris L.A., (2017), Removal of atenolol by adsorption - Study of kinetics and equilibrium, *Journal of Cleaner Production*, **154**, 214-219.

Hu Q., Zhang Z., (2019), Application of Dubinin-Radushkevich isotherm model at the solid/solution interface: A theoretical analysis, *Journal of Molecular Liquids*, **227**, 646-648

Johnson R. D., Arnold F. H., (1995), The Temkin isotherm describes heterogeneous protein adsorption, *Biochimica et Biophysica Acta (BBA)-Protein Structure and Molecular Enzymology*, **1247**, 293-297.

Kamiyama N., Panomsuwan G., Yamamoto E., Sudare T., Saito N., Ishizaki T., (2016), Effect of treatment time in the Mg(OH)2/Mg-Al LDH composite film formed on Mg alloy AZ31 by steam coating on the corrosion resistance, *Surface & Coatings Technology*, **286**, 172–177.

Meroufel B., Benali O., Benyahia M., Benmussa Y., Zenasni M.A., (2013), Adsorptive removal of anionic dye from aqueous solutions by Algerian kaolin: Characteristics, isotherm, kinetic and thermodynamic studies, *Journal of Materials and Environmental Science*, **4**, 482-491.

Namasivayam C., Sengeetha D., (2006), Removal of molybdate from water by adsorption onto $ZnCl_2$ activated coir pith carbon, *Bioresource Technology*, **97**, 1194-1200.

Paikaray S.M., Hendry J., Essilfie-Dughan J., (2013), Controls on arsenate, molybdate, and selenate uptake by hydrotalcite-like layered double hydroxides, *Chemical Geology*, **345**, 130–138.

Shin S.M., Senanayake G., Sohn J.-S., Kang J.-G., Yang D.-H., Kim T.-H., (2009), Separation of zinc from spent zinc-carbon batteries by selective leaching with sodium hydroxide, *Hydrometallurgy,* **96**, 349-353.

Tkac P., Paulenova A., (2008), Speciation of molybdenum (VI) in aqueous and organic phases of selected extraction systems, *Separation Science and Technology*, **43**, 2641-2657.

Turk T., Alp I., Deveci H., (2009), Adsorption of As(V) from water using Mg–Fe-based hydrotalcite (FeHT), *Journal of Hazardous Materials*, **171**, 665–670.

Vucelic M., Jones W., Moggridge, G.D., (1997), Cation ordering in synthetic layered double hydroxides, *Clays and Clay Minerals*, **45**, 803-813.

Wang J., Xu J., Xia J., Wu F., Zhang Y., (2018), A kinetic study of concurrent arsenic adsorption and phosphorus release during sediment resuspension, *Chemical Geology*, **495**, 67-75.

WHO, (2011), *Guidelines for drinking water quality*, Fourth edition, World Health Organization, On line at: https://www.who.int/water_sanitation_health/publications/drinking-water-quality-guidelines-4-including-1st-addendum/en/

Xiaoliang L., Gaoling W., Juan X., Fuding T., Hongping H., Chenchen Q., Hui Y., Jianxi Z., Runliang Z., Zonghua Q., Jing Z., (2017), Adsorption isotherm, mechanism, and geometry of Pb(II) on magnetites substituted with transition metals, *Chemical Geology*, **470**, 132-140.

Xie F., Cai T., Ma Y., Li H., Li C., (2009), Recovery of Cu and Fe from Printed Circuit Board waste sludge by ultrasound: Evaluation of industrial application, *Journal of Cleaner Production*, **17**, 1494-1498.

Yang Y., Yan X., Hu X., Feng R., Zhou M., Cui W., (2018), Development of zeolitic imidazolate framework-67 functionalized Co-Al LDH for CO_2 adsorption, *Colloids and Surfaces A: Physicochemical and Engineering Aspects*, **552**, 16-23.

Zhang X., Zhou L., Pi H., Guo S., Fu J., (2014), Performance of layered double hydroxides intercalated by a UV stabilizer in accelerated weathering and thermal stabilization of PVC, *Polymer Degradation and Stability*, **102**, 204–211.